

Biological Treatment of Poplar Wood with White-rot Fungus *Trametes hirsuta* C7784: Structural Elucidation of the Whole Lignin in Treated Wood

Hua Zhang,^a Sheng Yang,^{b,*} Xiang-Yang Sun,^a and Tong-Qi Yuan^{b,*}

Poplar wood was subjected to biological treatment with a white-rot fungus *Trametes hirsuta* C7784. The structural features of the lignin in the untreated and treated poplar wood samples were comparatively elucidated. Milled wood lignin (MWL) and residual enzymatic lignin (REL) fractions of each sample were sequentially isolated. The total pure yields of the isolated lignin fractions after white-rot fungus treatment exceeded 96% (based on the Klason lignin content), and thus, represented the whole lignin in the fungus-treated poplar wood. The structural features of the lignin fractions were quantitatively analyzed. β -O-4' structures were the most prominent linkage in the biologically treated wood, and there were more present than in the untreated wood. To this effect, the lignin in the fungus-treated poplar wood was easily degraded and removed under mild conditions, which is essential for subsequent conversion processes.

Keywords: White-rot fungus; Poplar wood; Whole lignin; Structural elucidation; Quantitative analysis

Contact information: a: College of Forestry, Beijing Forestry University, Beijing, 100083, China; b: Beijing Key Laboratory of Lignocellulosic Chemistry, Beijing Forestry University, Beijing, 100083, China; * Corresponding authors: yangsheng230@bjfu.edu.cn; ytq581234@bjfu.edu.cn

INTRODUCTION

The rapid depletion of fossil fuel resources and the environmental issues related to their consumption have made the search for alternative energy sources – from renewable feedstocks, for example – a critical endeavor (Jordan *et al.* 2012; Liu *et al.* 2012; Sindhu *et al.* 2016). Lignocellulosic materials, which consist of cellulose, hemicelluloses, and lignin, have considerable potential in the preparation of renewable energy. While research efforts have been devoted to converting lignocelluloses to bioethanol, the recalcitrance of lignocelluloses to processing, which is primarily caused by the rigid structure of lignin in the plant cell walls, significantly impedes their conversion (Sun and Cheng 2002; Berlin *et al.* 2006; Himmel *et al.* 2007; Munk *et al.* 2015). Pretreatment processes that ameliorate this recalcitrance include steam explosion, acid hydrolysis, alkaline hydrolysis, hydrothermal treatment, and biological treatment (Rabemanolontsoa and Saka 2015). According to the statistical data, pretreatment, as the first step towards conversion of lignocellulosic feedstocks to fuels and chemicals, makes up to one-third of the total production costs and remains one of the main barriers to commercial success (Saha *et al.* 2016). Compared with physical or chemical pretreatments, the biological method shows remarkable promise due to its mild process conditions, operational costs, and energy consumption coupled with enhanced environmental compatibility and sustainability (Sindhu *et al.* 2016).

White-rot fungi are the only known organisms that can completely break down lignin into carbon dioxide and water (Have and Teunissen 2001). These fungi are the most

promising organisms for delignifying or depolymerizing lignin in a variety of lignocellulosic materials (Dinis *et al.* 2009; Yang *et al.* 2010b; Saha *et al.* 2016). Fully eliminating lignin using white-rot fungi is not feasible for biofuel production because white-rot fungi treatment is an excessively slow process, and a large amount of the cellulose and hemicelluloses are consumed as carbon sources for fungal metabolism. While white-rot fungi can secrete all the enzymes (lignin peroxidase, manganese (II)-dependent peroxidase, laccase, cellulase, hemicellulases) needed to degrade lignocellulosic material components (de Menezes *et al.* 2009; Sunardi *et al.* 2016), the relatively high lignin content in biomass even after brief biological treatment still hinders enzymatic hydrolysis. For this reason, additional supplementary treatments are indispensable to successfully remove the lignin remaining in biologically treated biomass materials (Wan and Li 2012; Wang *et al.* 2013; Yang *et al.* 2013).

An efficient lignin removal procedure for biologically treated plant cell walls is essential for the success of subsequent conversion processes. Such processes are dependent on a comprehensive and detailed understanding of the structural features of lignin in biologically treated materials. Previous studies have primarily focused on milled wood lignin (MWL) (Yang *et al.* 2010a; Mao *et al.* 2013); however, due to its low yield, MWL does not appropriately represent the whole lignin in biologically treated plant cell walls. Additionally, the study of lignin in biologically treated residual wood meal after MWL extraction is rare.

In the present study, the MWL fractions isolated from untreated and white-rot-fungus-treated poplar wood, and the corresponding residual lignin fractions collected from the MWL extracted residue through a full enzymatic hydrolysis were also obtained. The structural features of the various isolated lignin samples were comparatively elucidated using gel permeation chromatography (GPC), component analysis, and quantitative two-dimensional heteronuclear single-quantum coherence (2D HSQC) NMR spectroscopy.

EXPERIMENTAL

Methods

Microorganism and inoculum preparation

Trametes hirsuta (a white-rot fungus) can produce laccase, which has been used for the biological bleaching of various pulps due to its favorable lignolytic ability (Kandioller and Christov 2001). In this study, *Trametes hirsuta* C7784 that was isolated from a live hardwood in Guangdong Province, China, was used. The fungus was maintained on 2% (w/v) malt extract agar plates at 4 °C in the laboratory until it was activated by applying 100 mL of a basic medium (*i.e.*, glucose 20 g/L, yeast extract 5 g/L, K₂HPO₄ 1 g/L, MgSO₄ 0.5 g/L, and vitamin B₁ 0.01 g/L). The mycelial pellets were constantly shaken on a rotary shaker at 28 °C for 5 days. Afterwards, 100 mL of distilled water was added, and the pellets were stirred for 30 s at 5000 rpm to obtain homogenous inocula. The isolated fungus has been identified prior to testing.

Biological treatment of poplar wood

A fast-growing, seven-year-old poplar tree (Triploid of *Populus tomentosa* Carr.) was harvested from the experimental farm of Beijing Forestry University (Beijing, China). The diameter of the poplar tree was about 20 cm, and the middle of the trunk of the poplar tree was obtained as material. The poplar wood was sun-dried and ground to wood powder.

The wood powder was firstly sieved with 60-mesh screen, and the wood powder, which passed the 60-mesh screen, was sieved with an 80-mesh screen. Then, the wood powder, which not passed the-80 mesh screen, was collected as raw material and the sample size of the raw material was 0.18 to 0.25 mm. For each run, a total of 10 g of raw material and 25 mL of distilled water were placed in a 250-mL Erlenmeyer flask. Samples were sterilized in an autoclave at 121 °C for 20 min before 5 mL of fungi inoculum was added to the flask. The strains were cultured for 4 or 8 weeks in a constant temperature (28 °C) and humidity environment. A non-inoculated sample served as the control.

Lignin isolation

Lignin fractions were isolated according to the scheme shown in Fig. 1. The biologically treated raw material was extracted with toluene/ethanol (2:1, v/v) in a Soxhlet extractor for 6 h, air-dried, and subsequently ball-milled as previously described (Yuan *et al.* 2011a). The materials were extracted in a 1,4-dioxane/water mixture (24:1, v/v) with a solid-to-liquid ratio of 1:10 (g/mL) for 24 h under a nitrogen atmosphere in the dark; the entire 1,4-dioxane/water extraction process was conducted twice. The combined extraction liquors were first concentrated to 50 mL using a rotary evaporator. Dissolved impurities were precipitated using 3 volumes of 95% ethanol to remove the hemicellulose fractions. After evaporating the ethanol, the 1,4-dioxane containing lignin was poured into a 50 volume of acetic acid/water mixture (9:1, v/v), and the lignin fraction was precipitated into the acidic water to obtain purified MWL.

The MWL fractions obtained from the control, 4-week fungus-treated, and 8-week fungus-treated poplar wood samples were labeled as MWL-0, MWL-4, and MWL-8, respectively. The residual wood meal after MWL extraction was washed with water and treated with Celluclast 1.5 L (Novozymes, Beijing, China). This cellulolytic enzyme had a filter paper activity of 70 FPU/g in an acetate buffer solution (pH 4.5) at 45 °C for 48 h. Cellulase was added at 70 FPU/g substrate with a 2% solid loading. After enzymatic hydrolysis, the solution was centrifuged, and the enzyme-treated precipitate was alternately washed with an acetate buffer solution (pH 4.5) and water until neutral pH was obtained. The entire enzymatic hydrolysis process was conducted twice to fully remove carbohydrate contaminants in the residues obtained from MWL fraction extraction. The residual enzyme lignin (REL) fractions obtained from the control, 4-week fungus-treated, and 8-week fungus-treated samples were labeled as REL-0, REL-4, and REL-8, respectively.

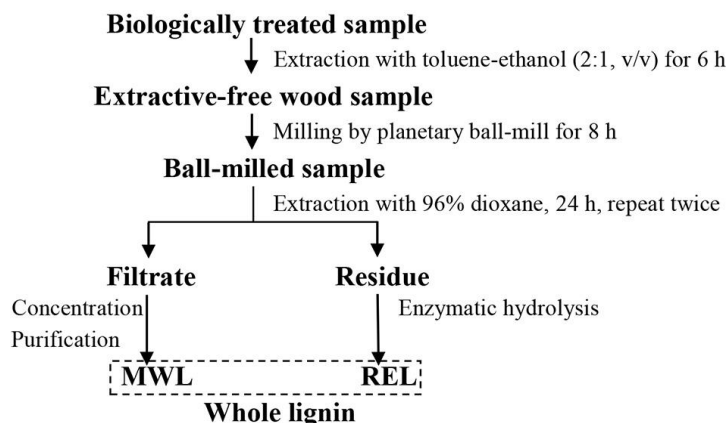


Fig. 1. Isolation of milled-wood lignin (MWL) and residual enzyme lignin (REL)

Biological treated sample analysis

The chemical compositions of the control and biologically treated poplar woods were determined according to the laboratory procedure of Sluiter *et al.* (2011). The analysis for each sample was run in duplicate, and average values were calculated as final results. To observe the morphologies of untreated and biologically treated wood samples, scanning electron microscopy (SEM) images were taken using a Hitachi S-3400N II (Hitachi, Tokyo, Japan) instrument operating at 10 kV and 81 mA, as previously described (Sun *et al.* 2014). The degree of crystallinity of the untreated and biologically treated poplar woods was determined by using X-ray diffractometry (XRD) (Shimadzu XRD-6000, Tokyo, Japan). The instrument was operated in reflection mode with a Cu- $K\alpha$ radiation source ($\lambda = 0.154$ nm) generated at 40 kV and 30 mA. The scattering angle (2θ) ranged from 5 to 35° at a scanning speed of 2°/min. The crystallinity index (*CrI*) was calculated as in Khan *et al.* (2014).

Lignin structural elucidation

The carbohydrate moieties associated with the obtained lignin fractions were determined by hydrolysis with diluted sulfuric acid (4% concentration) according to a method reported by Yuan *et al.* (2010), and analyzed by a high-performance anion-exchange detector chromatography (HPAEC) system (Dionex ICS3000, USA) with pulsed amperometric detector, AS50 autosampler, the CarboPac™ PA-20 column (4 × 250 mm, Dionex), and the guard PA-20 column (3 × 30 mm, Dionex). The analysis for each sample was run in duplicate, and average values were calculated as final results. The weight-average (M_w) and number-average (M_n) molecular weights of the lignin preparations were measured using gel permeation chromatography (GPC; Agilent 1200 series, Agilent Technologies, Santa Clara, USA). The GPC used a PL gel 10 mm Mixed-B 7.5 mm i.d. column and operated at conditions that have been previously published (Yuan *et al.* 2011b). Tetrahydrofuran (THF) was used as the eluent at a flow rate of 1 mL/min. To improve the solubility of the lignin fractions in the THF eluent, all isolated lignin samples were acetylated prior to GPC analysis. MWL acetylation was performed as reported by Pan *et al.* (2006), while REL acetylation was performed using the method of Lu and Ralph (2013). Two-dimensional heteronuclear single-quantum coherence (2D HSQC) NMR spectra of the MWLs and acetylated RELs (REL-Ac) were recorded using a Bruker AVIII 400 MHz spectrometer (Karlsruhe, Germany) operated at 25 °C using DMSO- d_6 solvent, as reported by Yuan *et al.* (2010). ^{31}P NMR spectra of the MWL fractions were recorded as described by Argyropoulos (1994).

RESULTS AND DISCUSSION

Analysis of Biological Pretreated Poplar Wood

The white fungi strain growing well on the poplar wood powder as shown in Fig. S1 (Supplementary material). The chemical constituents of the control and fungus-treated poplar wood samples are listed in Table 1. In the fungus-treated samples, a portion of the lignin and hemicelluloses were degraded, as expected; the relative cellulose content increased from 44.3% to 46.6% as the fungal treatment time progressed. These observations indicated that the white-rot fungus had degraded more lignin and hemicelluloses than cellulose. The degree of crystallinity of the fungus-treated samples

was higher than that of the untreated samples, as shown in Fig. S2 (Supplementary material). This observation suggested that part of the non-crystalline cellulose was degraded by the cellulase excreted by white-rot fungus. The delignification that occurred mainly affected the acid-insoluble lignin (*i.e.*, Klason lignin).

Table 1. Composition of Untreated and Biologically Treated Poplar Wood

	Cellulose (%)	Hemicellulose (%)	Acid-insoluble Lignin (%)	Acid-soluble Lignin (%)	Others ^b (%)
WT-0 ^a	44.3 (0.23) ^c	19.7 (0.25)	22.8 (0.39)	4.1 (0.26)	9.1 (0.22)
WT-4	45.5 (0.17)	18.0 (0.21)	18.8 (0.22)	4.3 (0.14)	13.4 (0.12)
WT-8	46.6 (0.34)	18.3 (0.12)	20.2 (0.22)	4.3 (0.35)	10.6 (0.37)

^a WT-0 represents control sample
^b This value was calculated by difference
^c The value in parenthesis is standard deviation

SEM analyses indicated that the impervious structure of the fibers of poplar wood was efficiently made more porous by the white-rot fungal treatment under the conditions used in this study. As shown in Fig. S3 (Supplementary material), after white-rot fungus treatment, the ordered arrangement of the fibers in the poplar wood was destroyed, and a large amount of microfibril was exposed. The fibers showed more pores and cracks as fungal treatment time increased. These structural changes could improve the efficiency of enzymatic hydrolysis of cellulose due to the increase of exposed contact area (Sindhu *et al.* 2016). These observations also provided evidence that the components of the plant cell walls are consumed by white-rot fungus during the allotted treatment time. The main purpose of this study was to investigate the structure of the lignin in the fungus-treated poplar wood without considering the material balances.

Table 2. Yield and Monosaccharide Content of MWL and REL

Sample	Yield (%) ^a		Total Sugar Content (%)	Sugars (%) ^b							
	With sugars	Without sugars		Rha	Ara	Gal	Glc	Man	Xyl	GlcA	GalA
MWL-0 ^c	20.7 (0.41) ^e	20.1 (0.35)	2.83 (0.31)	ND	ND	0.10	0.29	ND	2.03	0.41	ND
MWL-4	28.6 (0.39)	26.8 (0.62)	6.22 (0.37)	0.18	0.20	0.13	0.31	ND	4.94	0.47	ND
MWL-8	25.3 (0.52)	23.7 (0.69)	6.19 (0.29)	0.22	0.22	0.16	0.35	ND	4.61	0.63	ND
REL-0 ^d	75.9 (0.27)	67.1 (0.34)	11.62 (0.26)	0.36	0.54	1.06	4.22	1.40	3.20	0.78	0.06
REL-4	79.6 (0.34)	70.9 (0.36)	10.96 (0.33)	0.20	0.45	0.86	4.49	1.39	2.83	0.69	0.05
REL-8	82.6 (0.42)	72.3 (0.44)	12.41 (0.35)	0.19	0.48	0.92	5.58	1.46	3.03	0.68	0.07

^a Based on Klason (acid-insoluble) lignin of raw material
^b Abbreviations: Rha - rhamnose; Ara - arabinose; Gal - galactose; Glc - glucose; Man - mannose; Xyl - xylose; and GlcA - glucuronic acid
^c MWL-0 represents milled-wood lignin obtained from control sample
^d REL-0 represents residual enzyme lignin obtained from control sample
^e The value in parenthesis is standard deviation

Chemical Composition of Lignin Fractions

Results from component analyses of the isolated lignin fractions are reported in Table 2. The MWL fraction yield of the untreated and fungus-treated poplar woods were very low (from 20.1 to 26.8% based on the Klason lignin of poplar wood). Most lignin in the wood cell walls remained in the residue after MWL extraction. Thus, the lignin fractions in the residue of the white-rot-fungus-treated wood meal were also obtained after a thorough enzymatic hydrolysis; lignin yields in REL-0, REL-4, and REL-8 were 67.1, 70.9, and 72.3%, respectively. In all MWL fractions, the predominant monosaccharides were xylose, which was followed by glucuronic acid and glucose. The monosaccharides contained in the REL fractions were higher than those of the MWL fractions.

The lignin yield of the MWL-0 sample was lower than those of the MWL samples treated with white-rot-fungus; the sugar content of MWL-0 sample was also lower than that of any MWL fraction isolated from treated samples with white-rot fungus. This result reflected that the MWL fractions mainly originated from the middle lamellae of the wood cell walls (Sorvari *et al.* 1986), which was first degraded by ball milling and removed by subsequent extraction with 1,4-dioxane/water (24/1, v:v). Biological treatment allowed the lignin in the secondary layer of the wood cell walls to be isolated more easily through ball milling, and the hemicelluloses connected to this lignin fraction with lignin-carbohydrate complex (LCC) linkages were also isolated together. Most of the cellulose and hemicelluloses are located in secondary layer of the fiber walls, and the absolute content of lignin in the secondary layer is higher than that in the middle lamellae (Agarwal 2006). Compared with the yield of MWL-4, the yield of MWL-8 was relatively low, probably because some lignin was metabolized by white-rot fungi during eight weeks of treatment *versus* four weeks. With prolonged fungal treatment time, the pure yields of the REL fractions gradually increased; most lignin-carbohydrate complexes (LCCs) had been degraded by the white-rot fungus (Xiao *et al.* 2013), which resulted in less lignin being lost during hemicellulose isolation and MWL purification processes. The glucose content, followed by xylose, was the highest in all REL fractions. The relative content of glucose in the REL fractions increased as fungal treatment time increased. These observations were consistent with the results listed in Table 1.

Notably, the total pure yield of poplar lignin isolated from the white-rot fungus treatment was very high (*i.e.*, up to 96% based on the Klason lignin content). Thus, these samples could be regarded good representatives of whole lignin in biologically treated poplar woods.

Molecular Weight of Lignin Fractions

The values for weight average (M_w) and number-average (M_n) molecular weights calculated from the GPC curves (relative to polystyrene standards), as well as the values for polydispersity (M_w/M_n), for the MWL and REL fractions are shown in Table 3. The molecular weights of the MWL and REL fractions decreased after the white-rot fungus treatment, which indicated that the fungus effectively cleaved the linkages between the lignin units in the wood samples. The molecular weight of the MWL-8-Ac was higher than that of the MWL-4-Ac. The highly organized structures of the poplar cell walls were gradually deconstructed as the white-rot fungus treatment time increased, and thus more lignin fragments with relatively high molecular weights in biologically treated plant cell walls were easily isolated during the same ball milling conditions adopted by untreated plant cell wall ball milling process. In addition, the low polydispersity values of the MWL samples obtained from the poplar wood after white-rot fungus treatment indicated that the

lignin was mainly comprised of low molecular fractions; this observation provides further evidence that the lignin in the poplar cell walls was delignified during the treatment. The molecular weights of the REL fractions decreased as the treatment time increased, which revealed that the lignin in the wood cell walls were constantly degraded by the white-rot fungus.

Table 3. Weight-Average (M_w) Molecular Weight, Number-Average (M_n) Molecular Weight, and Polydispersity (M_w/M_n) of Acetylated Lignin Fractions

Sample	MWL-0-Ac	MWL-4-Ac	MWL-8-Ac	REL-0-Ac	REL-4-Ac	REL-8-Ac
M_w	4990	3320	3370	6070	5800	5430
M_n	1360	1280	1290	1380	1240	1300
M_w/M_n	3.67	2.59	2.61	4.40	4.68	4.18

Quantitative ^{31}P NMR Spectra

Quantitative ^{31}P NMR analysis was conducted to investigate the functional groups of the lignin fractions. Unfortunately, the high carbohydrate content of the REL fractions made it difficult to obtain reasonable ^{31}P NMR spectra. Thus, only the ^{31}P NMR spectra of the MWL fractions were recorded. Quantification was carried out *via* peak integration using cyclohexanol as the internal standard. Details regarding signal acquisition, assignment, and integration can be found elsewhere (Yuan *et al.* 2010). Table 4 provides the quantitative data on the distribution of the various hydroxyl functional groups of the MWL fractions.

Table 4. Hydroxyl Functional Groups of MWL as Determined by Quantitative ^{31}P -NMR Method (mmol/g)

Samples	Aliphatic OH	Syringyl OH		Guaiacyl OH		<i>p</i> -Hydroxy phenyl OH	Carboxylic OH	Total phenolic OH
		C ^a	NC ^b	C	NC			
MWL-0	3.65	0.16	0.43	0.13	0.65	0.02	0.13	1.39
MWL-4	4.70	0.09	0.29	0.08	0.48	0.15	0.17	1.09
MWL-8	4.89	0.13	0.28	0.10	0.50	0.16	0.22	1.17

^a Abbreviation: C - condensed
^b Abbreviation: NC - non-condensed

As shown in Table 4, the aliphatic hydroxyl group content of the MWLs from the fungal-treated samples increased considerably compared with that of the MWL obtained from untreated samples; this functional group increased gradually as the treatment time increased. This observation was likely caused by the cleavage of alkyl aryl ether bonds in the lignin during the biological treatment. The levels of syringial (S) and guaiacyl (G) phenolic hydroxyl groups in the MWL fractions decreased in the treated samples *versus* the untreated sample, whereas the levels *p*-hydroxyphenyl (H) phenolic hydroxyl groups increased.

This observation may be attributed to H lignin units being more easily isolated from the ball milling of poplar wood after white-rot fungus treatment. In addition, methoxyl removal occurred during white-rot fungus treatment may also contribute to this, as previously reported (Yang *et al.* 2010a; Mao *et al.* 2013). The total phenolic hydroxyl groups of the treated MWL fractions decreased, which is probably due to the metabolism

of this functional group by the white-rot fungus, as well as free radical coupling of phenolic hydroxyl groups that forms new lignin linkages. The phenolic hydroxyl groups of lignin are more active than the etherified phenolic groups during fungus treatment (Bugg *et al.* 2011; Munk *et al.* 2015). In addition, the increase of carboxyl groups in the treated MWL fractions may have been caused by the oxidation of the poplar lignin by various enzymes secreted by the white-rot fungi (Have and Teunissen 2001).

2D HSQC Spectra

To investigate the detailed structures of the fungal-treated lignin, all MWL and REL fractions were analyzed by 2D HSQC NMR. To remedy the poor solubility of the REL fractions in DMSO, the lignin fractions were acetylated prior to NMR analysis using a soluble solvent system (dimethyl sulfoxide/*N*-methylimidazole) and acetic anhydride as the acetylating agent. The side-chain (δ_C/δ_H 50 to 90/2.5 to 6.0) and aromatic (δ_C/δ_H 100 to 135/5.5 to 8.5) regions of the HSQC spectra of the MWL and REL-Ac fractions are shown in Figs. 2 and 3, respectively; the main substructures are depicted in Fig. 4.

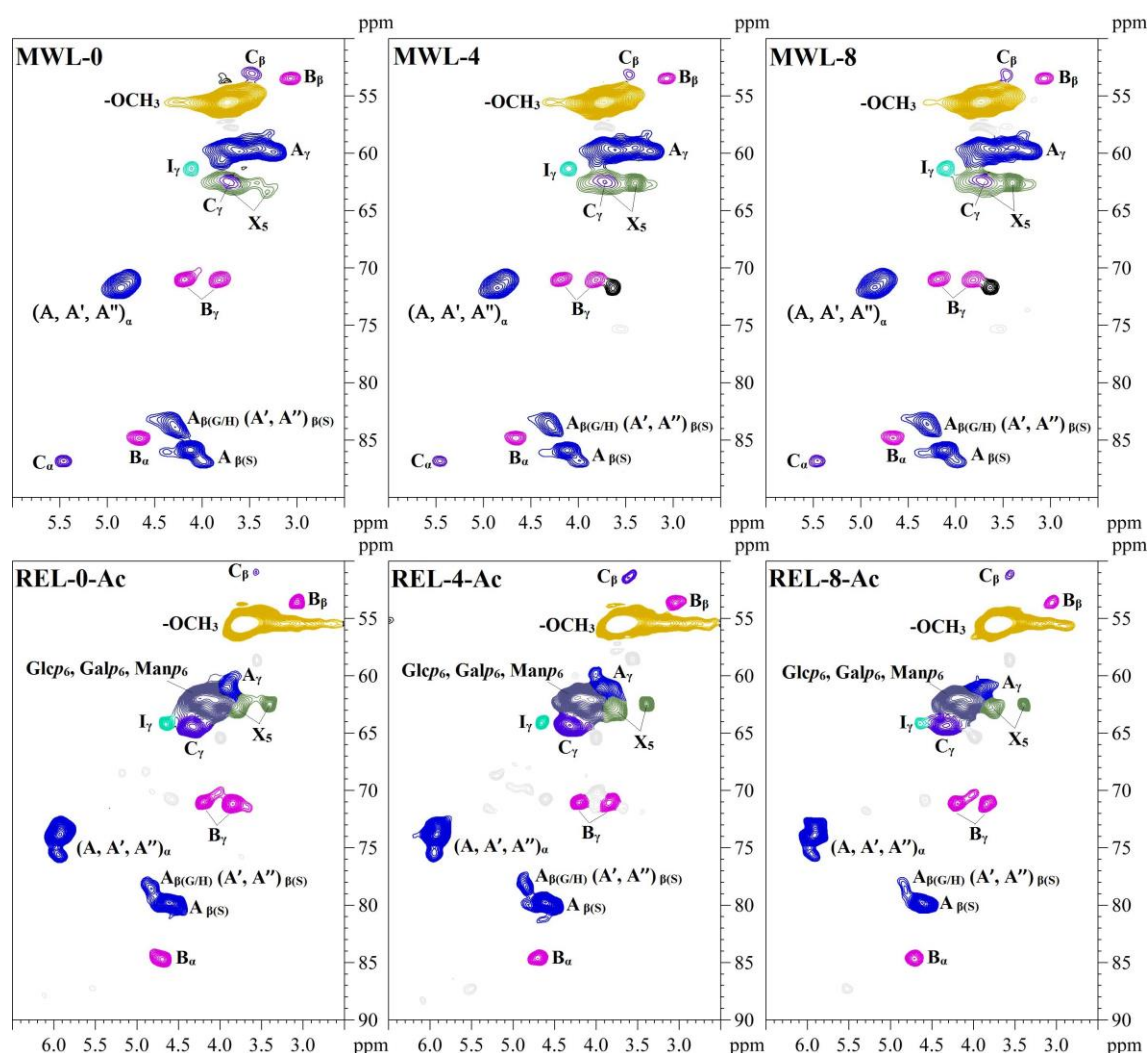


Fig. 2. Aliphatic (side-chain) regions of 2D ^{13}C - ^1H correlation (HSQC) spectra of milled-wood lignin (MWL) and residual enzyme lignin (REL) fractions. Symbols are taken from Fig. 4.

HSQC cross-signals of lignin and associated carbohydrates were assigned by comparison to published values (Lu and Ralph 2003; Balakshin *et al.* 2007; Kim and Ralph 2010; Xiao *et al.* 2013). The side-chain region of the 2D HSQC NMR spectra provided useful information regarding the inter-unit linkages present in lignin. As shown in Fig. 2, the side-chain regions of the isolated MWL fractions of untreated and fungus-treated wood in the HSQC spectra were similar. All spectra showed prominent signals corresponding to methoxyls (δ_C/δ_H 55.6/3.73) and β -O-4' aryl ether linkages. C_α - H_α correlations in β -O-4' substructures were observed at δ_C/δ_H 71.8/4.86 (structures A, A', and A''), whereas the C_β - H_β correlations corresponding to the *erythro* and *threo* forms of the syringyl β -O-4' substructures were present at δ_C/δ_H 85.9/4.12 and 86.8/3.99, respectively. These correlations shifted to δ_C/δ_H 83.9/4.29 in A structures linked to G and H lignin units, and γ -acylated β -O-4' aryl ether substructures (A') linked to S lignin units. C_γ - H_γ correlations in A structures were observed at δ_C/δ_H 59.5 to 59.7/3.40 to 3.63. In addition, strong signals for resinol (β - β') B substructures were observed with their C_α - H_α , C_β - H_β , and double C_γ - H_γ correlations at δ_C/δ_H 84.8/4.65, 53.5/3.06, and 71.0/4.18 and 3.82, respectively. The C_α - H_α and C_β - H_β correlations in phenylcoumaran (β -5', C) substructures were identified at δ_C/δ_H 86.8/5.46 and 53.3/3.46, respectively. Finally, the C_γ - H_γ correlations in *p*-hydroxycinnamyl alcohol end groups (I substructures) were observed at δ_C/δ_H 61.4/4.10 in the side-chain region of the MWL fractions. The C_5 - H_5 correlations of β -D-Xylp were observed at δ_C/δ_H 62.6/3.40 and 3.72. However, part of this signal is overlapped with C_γ - H_γ correlations of the phenylcoumaran substructures (C) around δ_C/δ_H 62.5/3.73.

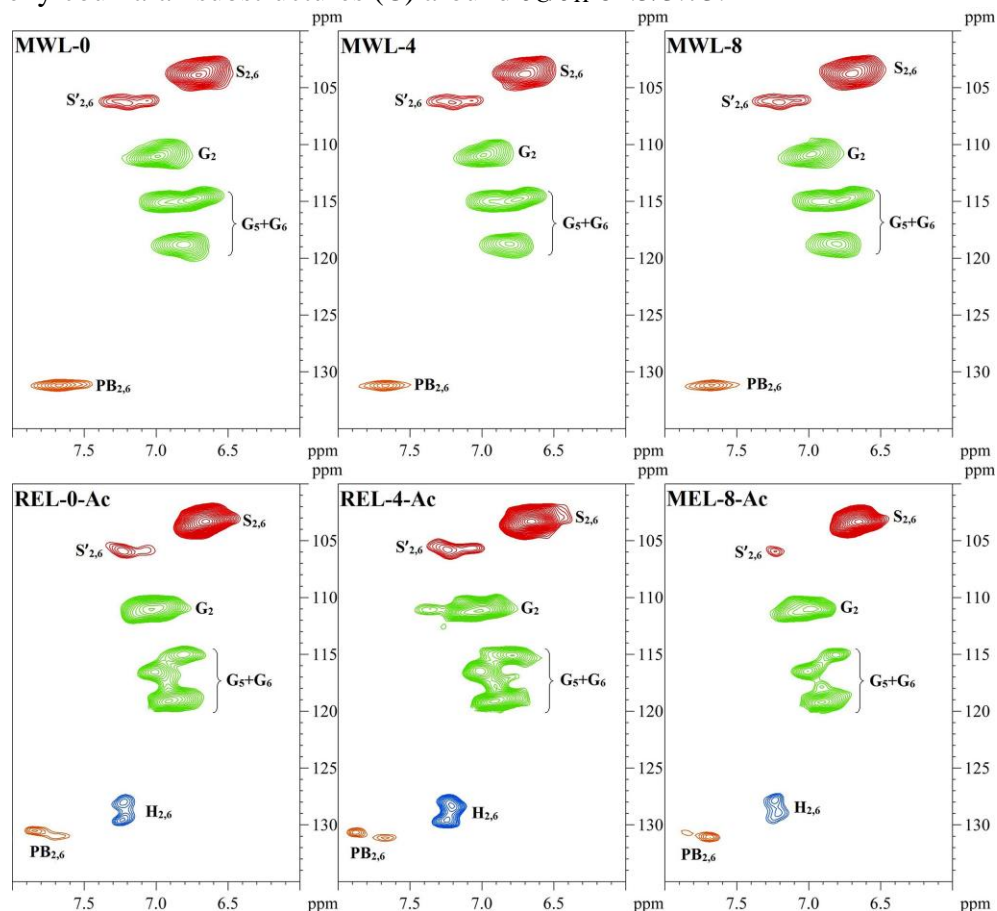


Fig. 3. Aromatic regions of 2D ^{13}C - ^1H correlation (HSQC) spectra of milled-wood lignin (MWL) and residual enzyme lignin (REL) fractions. Symbols are taken from Fig. 4.

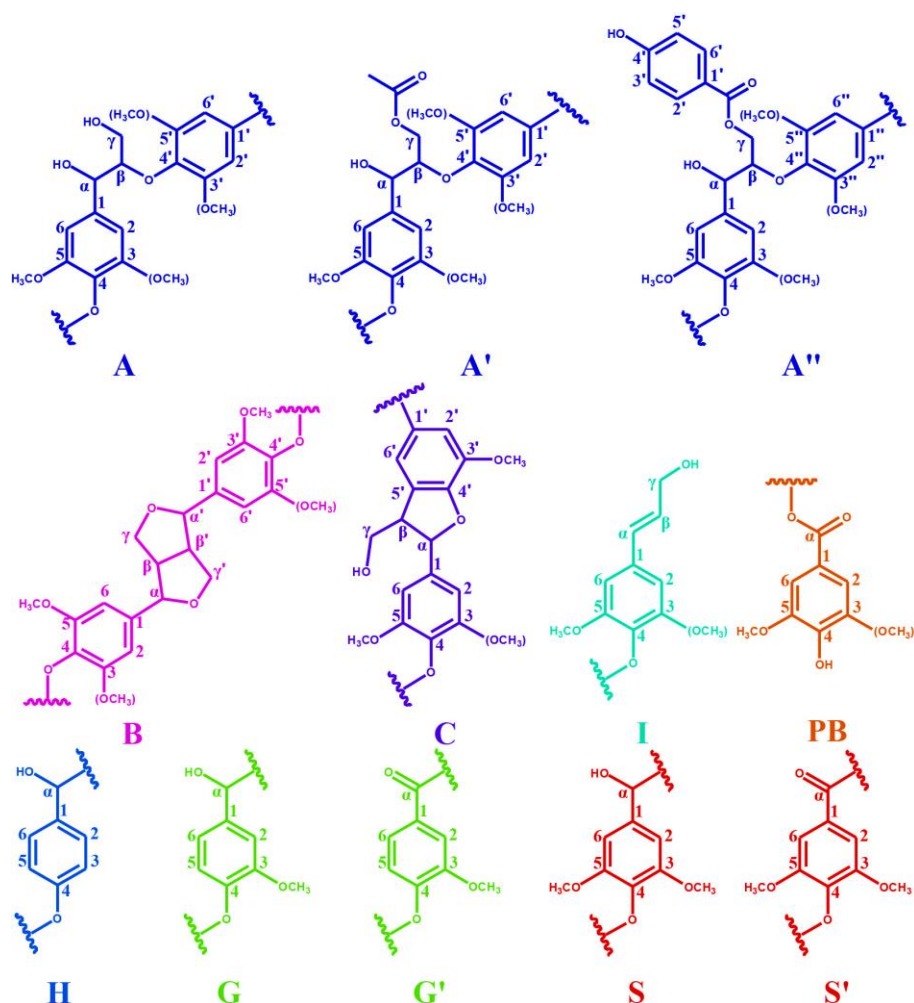


Fig. 4. Key structural details of milled-wood lignin (MWL) and residual enzyme lignin (REL): (A) β -O-4' aryl ether linkages with free -OH at the γ -carbon; (A') β -O-4' aryl ether linkages with acetylated -OH at γ -carbon; (A'') β -O-4' aryl ether linkages with *p*-hydroxybenzoated -OH at γ -carbon; (B) resinol substructures formed by β - β' linkages; (C) phenylcoumarane substructures formed by β -5'; (I) *p*-hydroxycinnamyl alcohol end groups; (PB) *p*-hydroxybenzoate substructures; (H) *p*-hydroxyphenyl units; (G) guaiacyl units; (S) syringyl units; (S') oxidized syringyl units with C_{α} ketone.

The main cross-signals in the aromatic region of the 2D HSQC spectra of the MWL fractions corresponded to the aromatic rings of syringyl (S) and guaiacyl (G) lignin units. The S units showed a prominent signal for the $C_{2/6}$ - $H_{2/6}$ correlations at δ_C/δ_H 103.8/6.71, whereas the $C_{2/6}$ - $H_{2/6}$ correlations in C_{α} -oxidized S units (S') were observed at δ_C/δ_H 106.2/7.23. The G units showed different correlations for C_2 - H_2 , C_5 - H_5 , and C_6 - H_6 at δ_C/δ_H 110.9/6.98, 114.9/6.77, and 119.0/6.80, respectively. Other signals in the aromatic regions were also identified and assigned to *p*-hydroxybenzoate substructures (PB). The $C_{2/6}$ - $H_{2/6}$ correlations of PB were observed at δ_C/δ_H 131.2/7.67.

The intensities of C_5 - H_5 correlations of β -D-Xylp in the MWL fractions obtained from the fungal-treated woods were relatively high, suggesting that the xylan content in the isolated MWL fractions from treated samples had increased. This result was consistent with the component analysis results. No H units were observed in the MWL fractions,

which seemed contradictory to the results of the quantitative ^{31}P NMR analysis. However, it should be highlighted that the specific existing site of the H type lignin unit in plant cell walls made it hard to be isolated by ball milling (Ikeda *et al.* 2002). Therefore, the signal belonging to H unit correlations could only be seen at the lower contour levels in the side-chain region of the spectra of MWL fractions (not shown).

The main inter-unit linkages and substructures in the 2D HSQC spectra of the acetylated REL fractions were similar to those of the MWL fractions, although the chemical shifts of some linkages changed after acetylation. There were extensive overlapped signals representing C₆-H₆ correlations of α -D-Glcp, β -D-Manp, and β -D-Galp at $\delta_{\text{C}}/\delta_{\text{H}}$ 61.0 to 62.6/3.5 to 4.3. The C₅-H₅ correlations of β -D-Xylp were identified at $\delta_{\text{C}}/\delta_{\text{H}}$ 62.6/3.40, in accordance with component analysis. In addition, C_{2/6}-H_{2/6} aromatic correlations from H units were clearly observed at $\delta_{\text{C}}/\delta_{\text{H}}$ 127.9/7.19 in all REL fractions; the intensity of these signals increased after white-rot fungus treatment. This also indicated that the H lignin units in poplar fiber wall were difficult to be isolated by ball milling. There were no obvious differences in the qualitative analyses of different lignin fractions obtained from untreated and fungal-treated poplar wood. Therefore, a quantitative analysis was necessary.

Quantitative Analysis of Lignin Structure

Table 5 presents the relative abundance of G and S lignin units, as well as the main lignin linkages (referred to as per 100 aromatic units (Ar)). These values were calculated from the 2D HSQC spectra of the lignin samples, which is based upon a previous publication (Wen *et al.* 2013). The β -O-4' linkages of the isolated MWL fractions from the fungal-treated wood increased compared with those of the isolated MWL fractions from the untreated sample; additionally, the S/G ratio increased with the treated samples. This indicated that the cell wall integrity was disrupted by the white-rot fungus, and as such, more lignin fractions with high β -O-4' content (mainly S type) were isolated by ball milling of poplar wood. No obvious changes were observed in the β - β' levels of treated and untreated MWL fractions, which differed from the results obtained by Mao *et al.* (2013). The relative abundance of β -5' linkages decreased to 3.31 per 100 Ar after four weeks of treatment, then increased to 4.11 per 100 Ar after eight weeks of treatment; this observation suggested that free radical coupling reactions had occurred with the lignin during the longer fungal treatment.

The S/G ratio of the REL-4-Ac changed slightly compared with the REL-0-Ac, whereas it decreased clearly with the REL-8-Ac. This observation implied that part of the S units was moved into the MWL fractions, and that some S units were converted to G units by demethoxylation reactions as treatment time increased. The β -O-4' levels of the REL-4-Ac was 65.95 per 100 Ar, which was lower than that of the REL-0-Ac; however, the β -O-4' levels increased to 79.91 per 100 Ar in the REL-8-Ac. This further suggested that lignin condensation of intermediate free radicals had occurred during the white-rot fungi treatment. The high β -O-4' levels in the REL fractions benefitted further lignin removal and cellulose conversion, because most of the lignin in plant cell walls were in REL fractions as shown in Table 2, and the β -O-4' linkages are easily broken (Parthasarathi *et al.* 2011). The β - β' content in the REL-0-Ac was higher than those in the other REL fractions treated with white-rot fungus. This was likely due to S unit removal, while the relatively high content of this lignin linkage in the REL-8-Ac may have been caused by lignin condensation of the intermediate free radicals. Obviously, the β -5' linkages increased in number in the REL fractions obtained from white-rot fungus treatment of the poplar

wood, which was probably due to increased G unit levels in the REL samples. The G unit is one of the prerequisites for β -5' formation (Wen *et al.* 2013).

The β -O-4' levels in the lignin obtained from the fungus-treated samples were higher overall than that in the untreated sample, which implied that the lignin in the treated wood was more readily degraded and removed. Thus, a simple and mild post-treatment with white-rot fungi may be sufficient and more effective to remove lignin from the plant cell walls, thereby making a biorefinery process more economical and achievable.

Table 5. Quantification of Lignin Fractions by 2D-HSQC NMR Method

Sample	β -O-4' ^a	β - β'	β -5'	S/G ^b
MWL-0	45.14	8.58	4.09	0.93
MWL-4	51.08	8.23	3.31	1.04
MWL-8	49.39	8.32	4.11	0.99
REL-0-Ac	68.64	12.48	0.35	0.87
REL-4-Ac	65.95	8.78	2.63	0.88
REL-8-Ac	79.91	11.49	2.68	0.78

^a Results expressed per 100 Ar based on quantitative 2D-HSQC spectra
^b S/G ratio obtained according to $S/G \text{ ratio} = 0.5/S_{2/6}/I_{G2}$

CONCLUSIONS

1. The impervious poplar wood cell walls were obviously disrupted by white-rot fungus *Trametes hirsuta* C7784, and the destructiveness increased with the treatment time prolonging.
2. The structural features of the lignin in wood changed after white-rot fungus treatment; lignin condensation of intermediate free radicals, which were produced during fungal treatment, likely occurred.
3. The β -O-4' structure was the most prominent linkage of the lignin obtained from biologically treated poplar wood; the content of this linkage was higher in the treated *versus* untreated wood samples.
4. The lignin in the fungus-treated poplar wood was easily degraded and removed under moderate conditions.

ACKNOWLEDGMENTS

The authors are grateful for support from the Fundamental Research Funds for the Central Universities (No.YX2015-03, 2015ZCQ-CL-02), State Forestry Administration (201404617), Special Fund for Forest Scientific Research in the Public Welfare (201504205), and Beijing Municipal Commission of Education (20131002201).

REFERENCES CITED

- Agarwal, U. P. (2006). "Raman imaging to investigate ultrastructure and composition of plant cell walls: Distribution of lignin and cellulose in black spruce wood (*Picea mariana*)," *Planta* 224(5), 1141-1153. DOI: 10.1007/s00425-006-0295-z
- Argyropoulos, D. S. (1994). "Quantitative phosphorus-31 NMR analysis of lignin, a new tool for the lignin chemist," *J. Wood Chem. Technol.* 14(1), 45-63. DOI: 10.1080/02773819408003085
- Balakshin, M. Y., Capanema, E. A., and Chang, H. M. (2007). "MWL fraction with a high concentration of lignin-carbohydrate linkages: Isolation and 2D NMR spectroscopic analysis," *Holzforschung* 61(1), 1-7. DOI: 10.1515/HF.2007.001
- Berlin, A., Balakshin, M., Gilkes, N., Kadla, J., Maximenko, V., Kubo, S., and Saddlera, J. (2006). "Inhibition of cellulase, xylanase and β -glucosidase activities by softwood lignin preparations," *J. Biotechnol.* 125(2), 198-209. DOI: 10.1016/j.jbiotec.2006.02.021
- Bugg, T. D. H., Ahmad, M., Hardiman, E. M., and Rahmanpour, R. (2011). "Pathways for degradation of lignin in bacteria and fungi," *Nat. Prod. Rep.* 28(12), 1883-1896. DOI: 10.1039/C1NP00042J
- de Menezes, C. R., Silva, Í. S., Pavarina, É. C., Guímaro Dias, E. F., Guímaro Dias, F., Grossman, M. J., and Durrant, L. R. (2009). "Production of xylooligosaccharides from enzymatic hydrolysis of xylan by the white-rot fungi *Pleurotus*," *Int. Biodeterior. Biodegrad.* 63(6), 673-678. DOI: 10.1016/j.ibiod.2009.02.008
- Dinis, M., Bezerra, R., Nunes, F., Dias, A., Guedes, C., Ferreira, L., Cone, J., Marques, G., Barros, A., and Rodrigues, M. (2009). "Modification of wheat straw lignin by solid state fermentation with white-rot fungi," *Bioresour. Technol.* 100(20), 4829-4835. DOI: 10.1016/j.biortech.2009.04.036
- Have, R. T., and Teunissen, P. J. M. (2001). "Oxidative mechanisms involved in lignin degradation by white-rot fungi," *Chem. Rev.* 101(11), 3397-3413. DOI: 10.1021/cr000115l
- Himmel, M. E., Ding, S. Y., Johnson, D. K., Adney, W. S., Nimlos, M. R., Brady, J. W., and Foust, T. D. (2007). "Biomass recalcitrance: Engineering plants and enzymes for biofuels production," *Science* 315(5813), 804-807. DOI: 10.1126/science.1137016
- Ikeda, T., Holtman, K., Kadla, J. F., Chang, H.-m., and Jameel H. (2002). "Studies on the effect of ball milling on lignin structure using a modified DFRC method," *J. Agric. Food Chem.* 50(1), 129-135. DOI: 10.1021/jf010870f
- Jordan, D. B., Bowman, M. J., Braker, J. D., Dien, B. S., Hector, R. E., Lee, C. C., Mertens, J. A., and Wagschal, K. (2012). "Plant cell walls to ethanol," *Biochem. J.* 442(2), 241-252. DOI: 10.1042/BJ20111922
- Kandioller, G., and Christov, L. (2001). "Evaluation of the delignification and bleaching abilities of selected laccases with HBT on different pulps," in: *Oxidative Delignification Chemistry Fundamentals and Catalysis*, D. S. Argyropoulos (ed.), Oxford University Press, New York, USA. DOI: 10.1021/bk-2001-0785.ch027
- Khan, E., Virojnagud, W., and Ratpukdi, T. (2004). "Use of biomass sorbents for oil removal from gas station runoff," *Chemosphere* 57(7), 681-689. DOI: 10.1016/j.chemosphere.2004.06.028
- Kim, H., and Ralph, J. (2010). "Solution-state 2D NMR of ball-milled plant cell wall gels in DMSO-*d*₆/pyridine-*d*₅," *Org. Biomol. Chem.* 8(3), 576-591. DOI: 10.1039/B916070A

- Liu, S. J., Lu, H. F., Hu, R. F., Shupe, A., Lin, L., and Liang, B. (2012). "A sustainable woody biomass biorefinery," *Biotechnol. Adv.* 30(4), 785-810. DOI: 10.1016/j.biotechadv.2012.01.013
- Lu, F. C., and Ralph, J. (2003). "Non-degradative dissolution and acetylation of ball milled plant cell walls: High-resolution solution-state NMR," *Plant J.* 35(4), 535-544. DOI: 10.1046/j.1365-313X.2003.01817.x
- Mao, J. Z., Zhang, X., Li, M. F., and Xu, F. (2013). "Effect of biological pretreatment with white-rot fungus *Trametes hirsuta* C7784 on lignin structure in *Carex meyeriana* Kunth," *BioResources* 8(3), 3869-3883. DOI: 10.15376/biores.8.3.3869-3883
- Munk, L., Sitarz, A. K., Kalyani, D. C., Mikkelsen, J. D., and Meyer, A. S. (2015). "Can laccases catalyze bond cleavage in lignin?," *Biotechnol. Adv.* 33(1), 13-24. DOI: 10.1016/j.biotechadv.2014.12.008
- Pan, X. J., Kadla, J. F., Ehara, K., Gilkes, N., and Saddler, J. N. (2006). "Organosolv ethanol lignin from hybrid poplar as a radical scavenger: Relationship between lignin structure, extraction conditions, and antioxidant activity," *J. Agric. Food Chem.* 54(16), 5806-5813. DOI: 10.1021/jf0605392
- Parthasarathi, R., Romero, R., Redondo, A., and Gnanakaran, S. (2011). "Theoretical study of the remarkably diverse linkages in lignin," *J. Phys. Chem. Lett.* 2(20), 2660-2666. DOI: 10.1021/jz201201q
- Rabemanolontsoa, H., and Saka, S. (2016). "Various pretreatments of lignocellulosics," *Bioresour. Technol.* 199, 83-91. DOI: 10.1016/j.biortech.2015.08.029
- Saha, B. C., Qureshi, N., Kennedy, G. J., and Cotta, M. A. (2016). "Biological pretreatment of corn stover with white-rot fungus for improved enzymatic hydrolysis," *Int. Biodeter. Biodegr.* 109, 29-35. DOI:10.1016/j.ibiod.2015.12.020
- Sindhu, R., Binod, P., and Pandey, A. (2016). "Biological pretreatment of lignocellulosic biomass – An overview," *Bioresour. Technol.* 199, 76-82. DOI: 10.1016/j.biortech.2015.08.030
- Sluiter, A., Hames, B., Ruiz, R., Scarlata, C., Sluiter, J., Templeton, D., and Crocker, D. (2011). *Determination of Structural Carbohydrates and Lignin in Biomass* (NREL/TP-510-42618), U. S. Department of Energy, National Renewable Energy Laboratory, Golden, USA.
- Sorvari, J., Sjöström, E., Klemola, A., and Laine, J. E. (1986). "Chemical characterization of wood constituents, especially lignin, in fractions separated from middle lamella and secondary wall of Norway spruce (*Picea abies*)," *Wood Sci. Technol.* 20(1), 35-51. DOI: 10.1007/BF00350693
- Sun, S. L., Wen, J. L., Ma, M. G., and Sun, R. C. (2014). "Enhanced enzymatic digestibility of bamboo by a combined system of multiple steam explosion and alkaline treatments," *Appl. Energ.* 136, 519-526. DOI: 10.1016/j.apenergy.2014.09.068
- Sun, Y., and Cheng, J. Y. (2002). "Hydrolysis of lignocellulosic materials for ethanol production: A review," *Bioresour. Technol.* 83(1), 1-11. DOI: 10.1016/S0960-8524(01)00212-7
- Sunardi, Tanabe, J., Ishiguri, F., Ohshima, J., Iizuka, K., and Yokota, S. (2016). "Changes in lignocellulolytic enzyme activity during the degradation of *Picea jezoensis* wood by the white-rot fungus *Porodaedalea pini*," *Int. Biodeter. Biodegr.* 110, 108-112. DOI:10.1016/j.ibiod.2016.02.022
- Wan, C., and Li, Y. (2012). "Fungal pretreatment of lignocellulosic biomass," *Biotechnol. Adv.* 30(6), 1447-1457. DOI: 10.1016/j.biotechadv.2012.03.003

- Wang, W., Yuan, T. Q., Cui, B. K., and Dai, Y. C. (2013). "Investigating lignin and hemicellulose in white rot fungus-pretreated wood that affect enzymatic hydrolysis," *Bioresour. Technol.* 134(April 2013), 381-385. DOI: 10.1016/j.biortech.2013.02.042
- Wen, J. L., Sun, S. L., Xue, B. L., and Sun, R. C. (2013). "Recent advances in characterization of lignin polymer by solution-state nuclear magnetic resonance (NMR) methodology," *Materials* 6(1), 359-391. DOI: 10.3390/ma6010359
- Xiao, L. P., Shi, Z. J., Bai, Y. Y., Wang, W., Zhang, X. M., and Sun, R. C. (2013). "Biodegradation of lignocellulose by white-rot fungi: Structural characterization of water-soluble hemicelluloses," *Bioenerg. Res.* 6(4), 1154-1164. DOI: 10.1007/s12155-013-9302-y
- Yang, H. Y., Wang, K., Wang, W., and Sun, R. C. (2013). "Improved bioconversion of poplar by synergistic treatments with white-rot fungus *Trametes velutina* D10149 pretreatment and alkaline fractionation," *Bioresour. Technol.* 130(Feb. 2013), 578-583. DOI: 10.1016/j.biortech.2012.12.103
- Yang, X. W., Ma, F. Y., Zeng, Y. L., Yu, H. B., Xu, C. Y., and Zhang, X. Y. (2010a). "Structure alteration of lignin in corn stover degraded by white-rot fungus *Irpex lacteus* CD2," *Int. Biodeter. Biodegr.* 64(2), 119-23. DOI: 10.1016/j.ibiod.2009.12.001
- Yang, X. W., Zeng, Y. L., Ma, F. Y., Zhang, X. Y., and Yu, H. B. (2010b). "Effect of biopretreatment on thermogravimetric and chemical characteristics of corn stover by different white-rot fungi," *Bioresour. Technol.* 101(14), 5475-5479. DOI: 10.1016/j.biortech.2010.01.129
- Yuan, T. Q., Xu, F., He, J., and Sun, R. C. (2010). "Structural and physicochemical characterization of hemicelluloses from ultrasound-assisted extractions of partially delignified fast-growing poplar wood through organic solvent and alkaline solutions," *Biotechnol. Adv.* 28(5), 583-593. DOI: 10.1016/j.biotechadv.2010.05.016
- Yuan, T. Q., Sun, S. N., Xu, F., and Sun, R. C. (2011a). "Characterization of lignin structures and lignin-carbohydrate complex (LCC) linkages by quantitative ¹³C and 2D HSQC NMR spectroscopy," *J. Agric. Food Chem.* 59(19), 10604-10614. DOI: 10.1021/jf2031549
- Yuan, T. Q., Sun, S. N., Xu, F., and Sun, R. C. (2011b). "Isolation and physicochemical characterization of lignins from ultrasound irradiated fast growing poplar wood," *BioResources* 6(1), 414-433. DOI: 10.15376/biores.6.1.414-433

Article submitted: May 9, 2016; Peer review completed: June 26, 2016; Revised version received and accepted: July 10, 2016; Published: July 14, 2016.

DOI: 10.15376/biores.11.3.7305-7321

APPENDIX

Supporting information

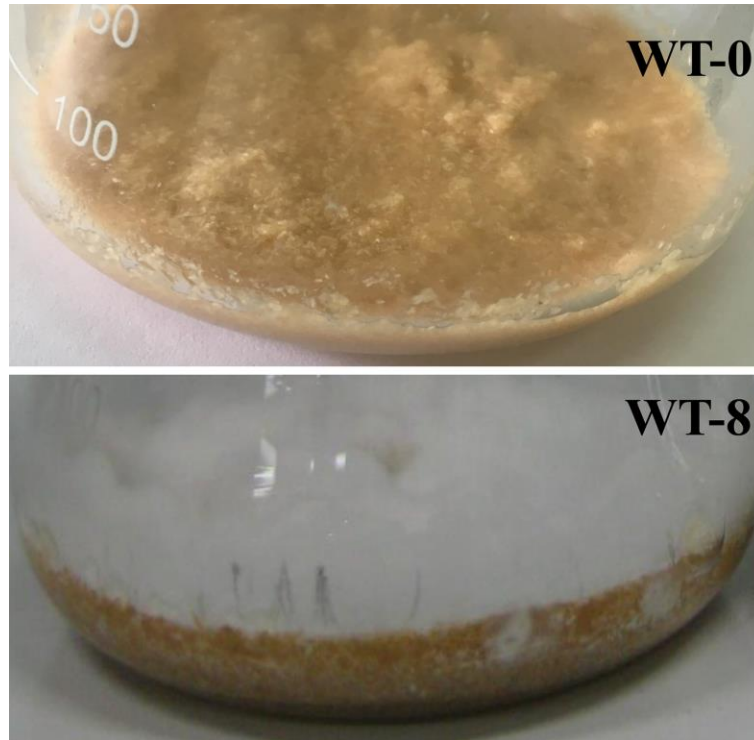


Fig. S1. 0-week (WT-0) and 8-week (WT-8) white-rot-fungus-treated poplar wood

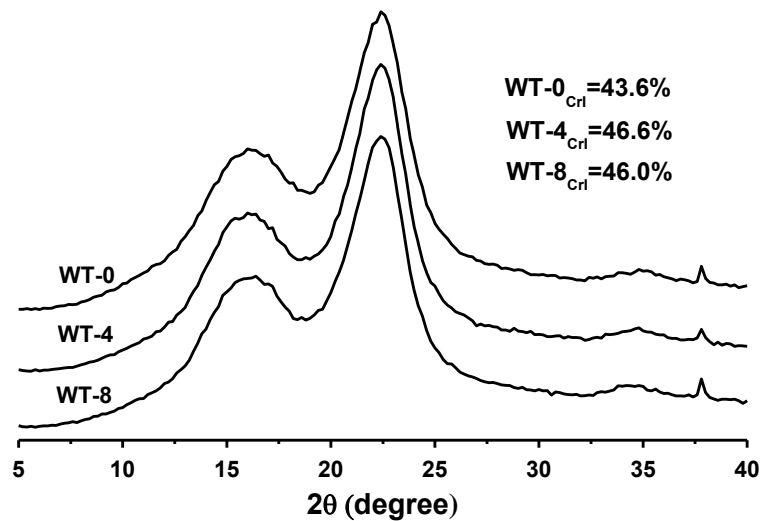


Fig. S2. X-ray diffraction patterns of untreated and white-rot-fungus-treated poplar woods: WT-0 is 0-week white-rot-fungus-treated poplar wood; WT-4 is 4-week white-rot-fungus-treated poplar wood; WT-8 is 8-week white-rot-fungus-treated poplar wood.

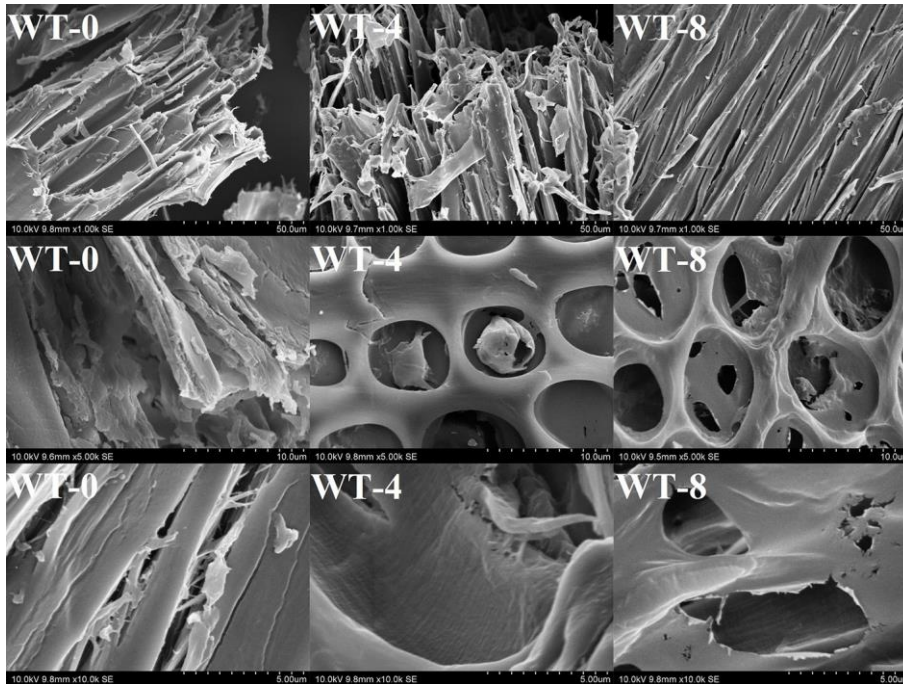


Fig. S3. Scanning electron microscope (SEM) images at various magnifications for untreated and white-rot-fungus-treated poplar woods. WT-0 is 0-week white-rot-fungus-treated poplar wood; WT-4 is 4-week white-rot-fungus-treated poplar wood; WT-8 is 8-week white-rot-fungus-treated poplar wood.